

High quantum efficiency InGaN/GaN multiple quantum well solar cells with spectral response extending out to 520 nm

R. M. Farrell, C. J. Neufeld, S. C. Cruz, J. R. Lang, M. Iza et al.

Citation: [Appl. Phys. Lett.](#) **98**, 201107 (2011); doi: 10.1063/1.3591976

View online: <http://dx.doi.org/10.1063/1.3591976>

View Table of Contents: <http://apl.aip.org/resource/1/APPLAB/v98/i20>

Published by the [American Institute of Physics](#).

Additional information on Appl. Phys. Lett.

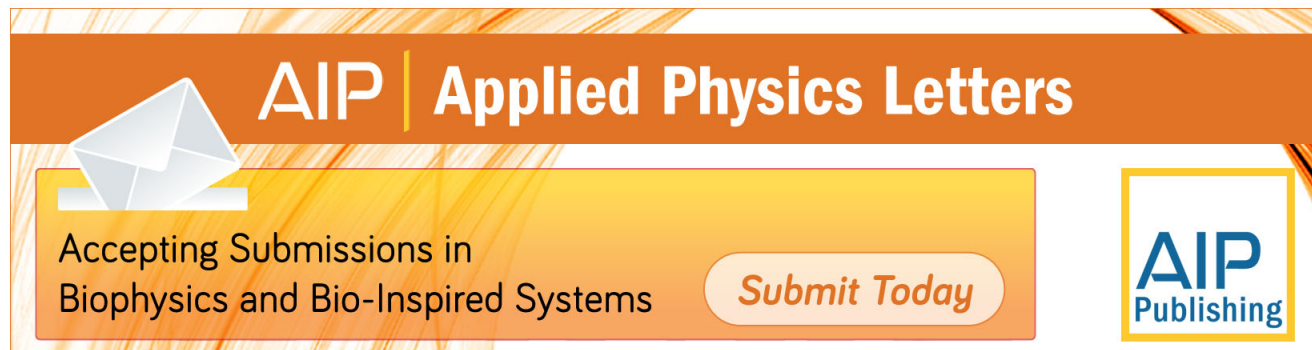
Journal Homepage: <http://apl.aip.org/>

Journal Information: http://apl.aip.org/about/about_the_journal

Top downloads: http://apl.aip.org/features/most_downloaded

Information for Authors: <http://apl.aip.org/authors>

ADVERTISEMENT

The advertisement banner features a background of orange and yellow diagonal stripes. At the top, the 'AIP Applied Physics Letters' logo is displayed in white. Below the logo, on the left, is a white envelope icon. To its right, the text 'Accepting Submissions in Biophysics and Bio-Inspired Systems' is written in black. Further right, a white button with the text 'Submit Today' in orange is shown. On the far right, the 'AIP Publishing' logo is displayed in blue and yellow.

AIP | Applied Physics Letters

Accepting Submissions in
Biophysics and Bio-Inspired Systems

Submit Today

AIP
Publishing

High quantum efficiency InGaN/GaN multiple quantum well solar cells with spectral response extending out to 520 nm

R. M. Farrell,^{1,a)} C. J. Neufeld,² S. C. Cruz,¹ J. R. Lang,¹ M. Iza,¹ S. Keller,² S. Nakamura,^{1,2} S. P. DenBaars,^{1,2} U. K. Mishra,² and J. S. Speck¹

¹Materials Department, University of California, Santa Barbara, California 93106, USA

²Department of Electrical and Computer Engineering, University of California, Santa Barbara, California 93106, USA

(Received 30 March 2011; accepted 25 April 2011; published online 18 May 2011)

We demonstrate high quantum efficiency InGaN/GaN multiple quantum well (QW) solar cells with spectral response extending out to 520 nm. Increasing the number of QWs in the active region did not reduce the carrier collection efficiency for devices with 10, 20, and 30 QWs. Solar cells with 30 QWs and an intentionally roughened p-GaN surface exhibited a peak external quantum efficiency (EQE) of 70.9% at 390 nm, an EQE of 39.0% at 450 nm, an open circuit voltage of 1.93 V, and a short circuit current density of 2.53 mA/cm² under 1.2 suns AM1.5G equivalent illumination. © 2011 American Institute of Physics. [doi:10.1063/1.3591976]

InGaN-based alloys have been utilized extensively for making high-performance light-emitting diodes (LEDs) and laser diodes with emission wavelengths ranging from the near UV to green regions of the optical spectrum.¹ More recently, InGaN-based alloys have also begun to receive considerable attention for photovoltaic applications.² This interest has been driven by the favorable physical properties of InGaN-based alloys for photovoltaic applications, including a direct band gap ranging from 0.64 eV for InN to 3.4 eV for GaN,^{3,4} high absorption coefficients of $\sim 10^5$ cm⁻¹ near the band edge,⁵ superior radiation resistance compared to other photovoltaic materials,^{2,4} and the potential for integration with existing silicon technology.⁶ Current state-of-the-art high-efficiency multijunction solar cells based on three junction GaInP/GaAs/Ge designs (with band gaps of 1.85 eV, 1.4 eV, and 0.67 eV, respectively) have attained conversion efficiencies of 41.6%, but future generation devices will require more junctions and subcells with larger band gaps to reach conversion efficiencies greater than 50%.⁷ These limitations indicate the tremendous potential of InGaN-based alloys for high-efficiency multijunction solar cells, especially for high-energy subcells with band gaps greater than 2.2 eV, for which few alternative materials currently exist.

Although high external quantum efficiencies (EQEs) have been demonstrated at wavelengths less than 420 nm for InGaN-based solar cells with relatively low indium content active regions,^{8,9} EQEs have been limited to less than 10% at wavelengths longer than 450 nm for InGaN-based solar cells with higher indium content active regions,¹⁰⁻¹² restricting the spectral response of all previously reported InGaN-based solar cells to regions of the solar spectrum with relatively low photon flux density. The difficulty in making devices with high indium content active regions is partly related to the large lattice mismatch between InN and GaN, necessitating the use of multiple quantum well (MQW) active region designs in InGaN-based solar cells with high indium content active regions.¹⁰⁻¹² In addition, unlike typical InGaN/GaN MQW LEDs, a relatively large number of highly strained QWs (e.g., 30+) are needed in InGaN/GaN MQW solar cells

to absorb a significant portion of the incident solar radiation and the effects of polarization need to be carefully managed to ensure efficient carrier collection,¹³ further complicating the materials growth and device design. In this letter, we effectively address these challenges and demonstrate high quantum efficiency InGaN/GaN MQW solar cells with spectral response extending out to 520 nm.

Metal-organic chemical-vapor deposition (MOCVD) was used to grow InGaN/GaN MQW solar cell structures on double-side-polished 50 mm (0001) sapphire substrates. The solar cell structures consisted of a 1 μ m unintentionally doped GaN template layer, a 2 μ m Si-doped n-GaN layer ([Si]= 6×10^{18} cm⁻³), a 10 nm highly Si-doped n⁺-GaN layer ([Si]= 2×10^{19} cm⁻³), a 10 to 30 period undoped MQW active region with 2.2 nm In_{0.28}Ga_{0.72}N QWs and 8 nm GaN barriers, a 40 nm highly Mg-doped smooth p⁺-GaN layer ([Mg]= 5×10^{19} cm⁻³), a 30 nm Mg-doped smooth p-GaN layer ([Mg]= 2×10^{19} cm⁻³), a 0–300 nm Mg-doped intentionally roughened p-GaN layer ([Mg]= 2×10^{19} cm⁻³), and a highly Mg-doped p⁺-GaN contact layer. The general structure of the solar cells is illustrated in the cross-sectional schematic shown in Fig. 1(a). Four solar cell samples, labeled A, B, C, and D, were grown for compari-

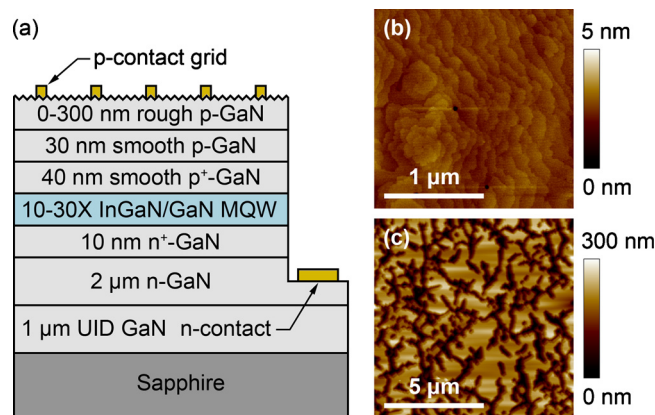


FIG. 1. (Color online) (a) Cross-sectional schematic of the general device structure. (b) 2 μ m \times 2 μ m AFM image of the surface of sample C. (c) 10 μ m \times 10 μ m AFM image of the surface of sample D.

^{a)}Electronic mail: rmf@ece.ucsb.edu.

son. Samples A, B, and C contained 10 QWs, 20 QWs, and 30 QWs, respectively, with 70 nm of smooth p-GaN on top of each active region, followed by a highly doped p⁺-GaN contact layer. Sample D contained 30 QWs with 70 nm of smooth p-GaN on top of the active region, followed by 300 nm of intentionally roughened p-GaN and a highly doped p⁺-GaN contact layer. The highly Si-doped and highly Mg-doped layers adjacent to the active region were necessary for screening the polarization-induced electric fields in the QWs,¹³ which are in the opposite direction of the p-n junction depletion field for p-side-up Ga-polar solar cells and can inhibit carrier collection if not properly accounted for in the device design.¹⁴

Following the MOCVD growth, the samples were characterized by atomic force microscopy (AFM) with a Digital Instruments Dimension 3000 AFM and by x-ray diffraction (XRD) with a PANalytic MRD PRO diffractometer. The absorption spectra of the unprocessed wafers were measured using a Shimadzu UV-3600 UV-VIS-NIR spectrophotometer coupled with an integrating sphere, as described elsewhere.¹⁵ After completing the material characterization, the samples were processed into solar cells using standard contact lithography processes. The final device structure consisted of 1 mm × 1 mm mesas, 30/300 nm Pd/Au p-contact grids on the top of each mesa with a center-to-center grid spacing of 200 μm, and 30/300 nm Al/Au n-contacts around the base of each mesa. After completion of the device fabrication, the devices were measured by on-wafer probing at room temperature. Dark and illuminated current density versus voltage (*J*-*V*) measurements were taken with a Keithley 2635 source meter. Broadband illumination was provided by an unfiltered 300 W Oriel Xe lamp with an equivalent AM1.5G illumination intensity of approximately 1.2 suns, as determined by integration of the EQE spectra over the AM1.5G solar spectrum. EQE measurements were collected under monochromatic illumination using the same Oriel Xe lamp in conjunction with an Oriel 260 monochromator and were calibrated with a reference Si photodetector.

AFM images are presented in Figs. 1(b) and 1(c) for the smooth and intentionally roughened p-GaN surfaces of samples C and D, respectively. A roughened p-GaN surface decreases the reflection at the p-GaN/air interface and increases the path length of the light through the active region, increasing the total light absorbed by the solar cell.¹⁵ The intentionally roughened surface was achieved by growing the p-GaN at a relatively low growth temperature and a relatively high growth rate, resulting in the formation of v-defects under kinetically limited growth conditions.¹⁶ As shown by the 2 μm × 2 μm AFM image (5 nm data scale) of sample C in Fig. 1(b), the smooth p-GaN surface was characterized by step flow growth and a root-mean-squared (RMS) roughness of ~0.5 nm over a typical 2 μm × 2 μm area. In contrast, as shown by the 10 μm × 10 μm AFM image (300 nm data scale) of sample D in Fig. 1(c), the intentionally roughened p-GaN surface was characterized by a high density of very deep v-defects and a significantly larger RMS roughness of ~75 nm over a typical 2 μm × 2 μm area.

Figure 2(a) depicts XRD ω -2 θ scans taken across the (0002) reflection for samples A, B, C, and D. The vertical dotted lines on the zeroth and first order superlattice peaks signify that the period and average composition of the

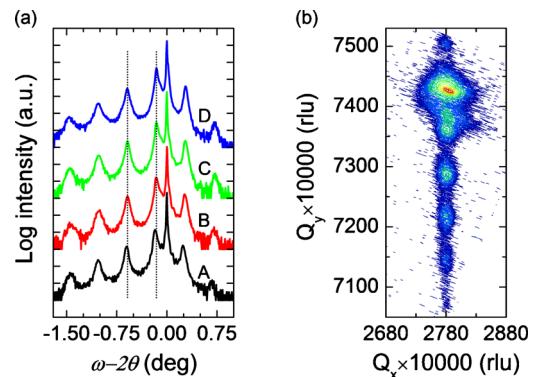


FIG. 2. (Color online) (a) XRD ω -2 θ scans taken across the (0002) reflection for samples A, B, C, and D. (b) XRD reciprocal space map taken around the asymmetric (105) reflection for sample D.

InGaN/GaN MQW active regions were very similar for all four samples. Figure 2(b) shows an XRD reciprocal space map taken around the asymmetric (105) reflection for sample D. The vertical alignment of the various superlattice peaks with the GaN peak indicates that the 30 period InGaN/GaN MQW was coherently strained to the GaN template, demonstrating that it is possible to grow coherently strained high indium content InGaN/GaN MQW solar cells with a large number of periods.

Following the material characterization and device fabrication, all samples were tested by on-wafer probing to determine how the number of quantum wells and surface morphology affected the device performance. EQE spectra for samples A, B, C, and D and absorption spectra for samples A, B, and C are presented in Fig. 3(a). Absorption data is not presented for sample D, though, because scattering from the rough p-GaN surface caused a portion of the light to propagate laterally in the smooth double-side-polished sapphire substrate, reducing the light collected by the integrating

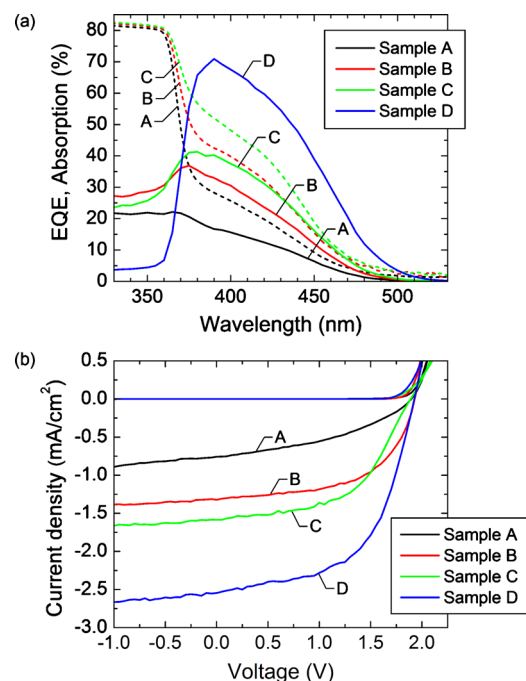


FIG. 3. (Color online) (a) Dependence of EQE (solid lines) and absorption (dashed lines) on wavelength for samples A, B, C, and D. (b) *J*-*V* curves for samples A, B, C, and D.

TABLE I. Summary of device performance metrics for samples A, B, C, and D.

| Sample | Number of QWs | p-GaN morphology | Peak EQE (%) | EQE at 450 nm (%) | IQE at 400 nm (%) | V_{oc} (V) | J_{sc} (mA/cm ²) | FF (%) |
|--------|---------------|------------------|--------------|-------------------|-------------------|--------------|--------------------------------|--------|
| A | 10 | Smooth | 22.1 | 6.4 | 61.0 | 1.90 | 0.76 | 40.2 |
| B | 20 | Smooth | 36.9 | 12.0 | 76.8 | 1.93 | 1.33 | 56.0 |
| C | 30 | Smooth | 41.3 | 16.2 | 77.9 | 1.89 | 1.57 | 53.7 |
| D | 30 | Rough | 70.9 | 39.0 | ... | 1.93 | 2.53 | 56.4 |

sphere and limiting the accuracy of the measurement.¹⁵ A comparison of the absorption and EQE spectra for samples A, B, and C shows that the internal quantum efficiency (IQE) did not decrease with an increasing number of QWs in the active region, indicating that increasing the number of QWs did not adversely affect the carrier collection efficiency. Similar trends have also been reported for GaAs-based MQW solar cells with up to 50 In_{0.1}Ga_{0.9}As QWs.¹⁷ Although accurate absorption data was not available for sample D, a comparison of the EQE spectra for samples C and D shows that intentionally roughening the p-GaN surface roughly doubled the EQE for wavelengths longer than the absorption edge of GaN. Table I contains a summary of the peak EQE and the EQE at 450 nm for all four samples and an estimate of the IQE at 400 nm for samples A, B, and C. Sample A, which only had 10 QWs and closely resembled the structure of a commercial green InGaN/GaN LED, exhibited a relatively low peak EQE of 22.1% at 365 nm and an even lower EQE of 6.4% at 450 nm. In contrast, sample D, which had 30 QWs and an intentionally roughened p-GaN surface, exhibited a relatively high peak EQE of 70.9% at 390 nm, a significantly improved EQE of 39.0% at 450 nm, and spectral response extending out to 520 nm.

Finally, dark and illuminated J - V measurements are depicted in Fig. 3(b) along with a summary of the open circuit voltage (V_{oc}), the short circuit current density (J_{sc}), and the fill factor (FF) in Table I. Measured FFs were similar for all samples and ranged from 50% to 60%, with the exception of sample A, which was only 40.2%. The reason why these FFs are significantly lower than the FFs previously reported (~80%) for InGaN-based solar cells with lower indium content active regions¹⁵ is not clear at present and is a subject of further investigation. While the V_{oc} was fairly consistent for all four samples, varying only slightly from 1.89 to 1.93 V, the J_{sc} increased dramatically with an increasing number of QWs and an increase in the surface roughness of the p-GaN layer, ranging from 0.76 mA/cm² for sample A to 2.53 mA/cm² for sample D, in agreement with the trends observed in the EQE spectra.

In summary, we have demonstrated high quantum efficiency InGaN/GaN MQW solar cells with spectral response extending out to 520 nm. Starting with a structure that closely resembled a commercial green InGaN/GaN LED but functioned poorly as a solar cell (sample A), we showed how increasing the number of QWs in the active region and roughening the surface of the p-GaN could significantly improve device performance. Solar cells with 30 QWs and an intentionally roughened p-GaN surface exhibited a peak

EQE of 70.9% at 390 nm, an EQE of 39.0% at 450 nm, a V_{oc} of 1.93 V, and a J_{sc} of 2.53 mA/cm² under 1.2 suns AM1.5G equivalent illumination.

This work was supported by the Center for Energy Efficient Materials (CEEM) at UCSB, an Energy Frontier Research Center funded by the U.S. DOE, the DARPA High Performance InGaN-Based Solar Cells Program, the California Advanced Solar Technologies Institute (CAST), and the Solid State Lighting and Energy Center (SSLEC). A portion of this work was done in the UCSB nanofabrication facility, part of the NSF NNIN network, as well as the UCSB MRL, which is supported by the NSF MRSEC program. The sapphire substrates and the trimethylindium metalorganic sources used for this study were provided by Namiki Precision Jewel and Sonata LLC, respectively.

¹M. R. Krames, O. B. Shchekin, R. Mueller-Mach, G. O. Mueller, L. Zhou, G. Harbers, and M. G. Craford, *J. Disp. Technol.* **3**, 160 (2007).

²J. Wu, W. Walukiewicz, K. M. Yu, W. Shan, J. W. Ager, E. E. Haller, H. Lu, W. J. Schaff, W. K. Metzger, and S. Kurtz, *J. Appl. Phys.* **94**, 6477 (2003).

³J. Wu, W. Walukiewicz, K. M. Yu, J. W. Ager, E. E. Haller, H. Lu, W. J. Schaff, Y. Saito, and Y. Nanishi, *Appl. Phys. Lett.* **80**, 3967 (2002).

⁴J. Q. Wu, *J. Appl. Phys.* **106**, 011101 (2009).

⁵A. David and M. J. Grundmann, *Appl. Phys. Lett.* **97**, 033501 (2010).

⁶L. A. Reichertz, I. Gherasoiu, K. M. Yu, V. M. Kao, W. Walukiewicz, and J. W. Ager, *Appl. Phys. Express* **2**, 122202 (2009).

⁷D. J. Friedman, *Curr. Opin. Solid State Mater. Sci.* **14**, 131 (2010).

⁸O. Jani, I. Ferguson, C. Honsberg, and S. Kurtz, *Appl. Phys. Lett.* **91**, 132117 (2007).

⁹C. J. Neufeld, N. G. Toledo, S. C. Cruz, M. Iza, S. P. DenBaars, and U. K. Mishra, *Appl. Phys. Lett.* **93**, 143502 (2008).

¹⁰R. Dahal, B. Pantha, J. Li, J. Y. Lin, and H. X. Jiang, *Appl. Phys. Lett.* **94**, 063505 (2009).

¹¹K. Y. Lai, G. J. Lin, Y. L. Lai, Y. F. Chen, and J. H. He, *Appl. Phys. Lett.* **96**, 081103 (2010).

¹²Y. Kuwahara, T. Fujii, T. Sugiyama, D. Iida, Y. Isobe, Y. Fujiyama, Y. Morita, M. Iwaya, T. Takeuchi, S. Kamiyama, I. Akasaki, and H. Amano, *Appl. Phys. Express* **4**, 021001 (2011).

¹³C. J. Neufeld, S. C. Cruz, R. M. Farrell, M. Iza, J. R. Lang, S. Keller, S. Nakamura, S. P. DenBaars, J. S. Speck, and U. K. Mishra, "Effect of doping and polarization on carrier collection in InGaN quantum well solar cells," *Appl. Phys. Lett.* (to be published).

¹⁴J. J. Wierer, A. J. Fischer, and D. D. Koleske, *Appl. Phys. Lett.* **96**, 051107 (2010).

¹⁵E. Matioli, C. Neufeld, M. Iza, S. C. Cruz, A. A. Al-Heji, X. Chen, R. M. Farrell, S. Keller, S. DenBaars, U. Mishra, S. Nakamura, J. Speck, and C. Weisbuch, *Appl. Phys. Lett.* **98**, 021102 (2011).

¹⁶X. H. Wu, C. R. Elsass, A. Abare, M. Mack, S. Keller, P. M. Petroff, S. P. DenBaars, J. S. Speck, and S. J. Rosner, *Appl. Phys. Lett.* **72**, 692 (1998).

¹⁷D. B. Bushnell, T. N. D. Tibbits, K. W. J. Barnham, J. P. Connolly, M. Mazzer, N. J. Ekins-Daukes, J. S. Roberts, G. Hill, and R. Airey, *J. Appl. Phys.* **97**, 124908 (2005).